Analyzing the root cause of critical self-excited cutting or friction induced vibrations considering multiple nonlinearities

V. Kulke [1], G. Ostermeyer [1], H. Reckmann [2], A. Hohl [2]
[1] TU Braunschweig, Institute of Dynamics and Vibrations,
Schleinitzstr. 20, D-38106, Braunschweig, Germany
e-mail: **gp.ostermeyer@tu-bs.de**

[2] Baker Hughes,
Baker-Hughes-Str. 1, D-29221, Celle, Germany

Abstract
Self-excited vibrations can negatively affect the system performance in various engineering applications. To effectively implement suitable countermeasures such as design changes or the installation of dampers, the root cause of the self-excitation must be analyzed. In this work, a method to determine the nonlinear characteristic of the force in complex contacts with friction is introduced. For this purpose, the influence of various nonlinear force components on the stability and system response are discussed and the dynamic behavior of the resulting vibrations are shown. An algorithm to analyze the energy input/output into the self-excited mode using measurement data and a suitable model of the considered structure is presented. By relating the resulting energy change to contact and operational parameters such as normal force and contact velocity as well as modal parameters such as amplitude, mode shape and natural frequency, the nonlinear contact force characteristic is determined.

1 Introduction

Vibrations occur in numerous technical applications [1, 2] and can lead to comfort, performance and reliability problems [3]. Apart from parameter excitation and external excitation, self-excitation takes an important role in systems with contacting surfaces, e.g. in systems with cutting of friction contacts [4]. In the case of self-excitation, the dynamic system periodically extracts energy from an energy source through a self-generating process. If the energy supplied by the self-excitation is higher than the energy dissipated through damping, unstable self-excited oscillations occur. The resulting vibrations correspond to modes of the structure. In the literature, mode coupling, regenerative effects, and nonlinear contact force characteristics are often described as the root causes of self-excited oscillations [5]. In numerous technical applications ranging from brake squeal [4, 6] and curve squealing of trains [7] to chatter vibration in machining tools [8] and the bit-rock interaction in drilling systems [9, 10] self-excited vibration occur. Methods to characterize and quantify the self-excitation have to be developed in order to reduce critical oscillations. Especially in drill string dynamics, the different influences of fluid, cutting and frictional forces as well as the changes in the contact properties, e.g. change of the drilled rock, effect the self-excitation and thus the dynamic motion of the structure. Furthermore, the observability of the excitation process is severely limited. Thus, effective methods to determine the nonlinear contact force characteristics in the bit-rock interaction during the drilling process have to be developed.

2 Analyzing self-excited vibrations

The nonlinear contact force characteristic is one of the most common causes of self-excitation in structures with cutting or friction contacts. This nonlinear characteristic is a consequence of the superposition of various linear and nonlinear forces. The interaction of friction/cutting forces and fluid forces is commonly described via

$$\mu(v) = \frac{2}{\pi} atan\left(\frac{\pi}{2} Sv\right)\left(\underbrace{(\mu_H - \mu_C)e^{-\left|\frac{v}{v_S}\right|}}_{\text{I}} + \underbrace{\mu_C}_{\text{II}} + \underbrace{b_S|v|}_{\text{III}}\right) \tag{1}$$

and leads to a nonlinear force characteristic (Figure 1, top) similar to the well-known Stribeck curve with constant parameters $\mu_H, \mu_C, b, v_S,$ and S.

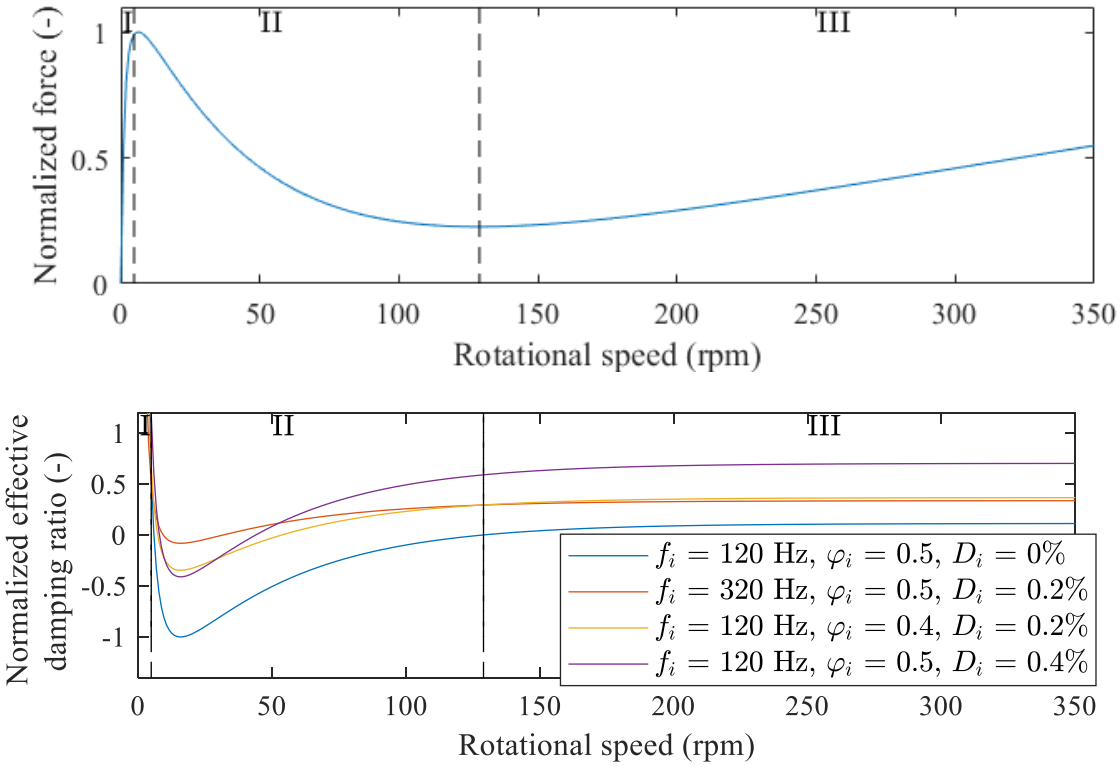

Figure 1: Normalized nonlinear torque characteristic (top) and corresponding normalized effective damping ratio for various modes (bottom)

The resulting force characteristic curve shows three distinctive ranges depending on the velocity dependency of the nonlinear contact forces which can be attributed to the force components in Equation 1. In the first range (I), at low speeds, the sticking component of the force dominates the system response. As the speed in the contact increases, sliding is getting dominant and the force in the second range (II) decreases until a minimum is reached. In the third range (III), the fluid portion of the contact becomes more dominant, and thus the force increases with the relative velocity in the contact. Depending on the slope of the torque characteristic with respect to the relative velocity in the contact, modes are stable or unstable [9]. This stability can be determined via the effective damping

$$D_{\text{eff},i} = \frac{\sum \Delta E}{2\omega_{0,i} \int_0^T \dot{q}_i^2 dt} = \frac{\Delta E_i + \Delta E_{\text{sl},i}}{2\pi\omega_{0,i}^2 \hat{q}_i^2} = D_i + D_{\text{sl},i}, \tag{2}$$

which corresponds to the sum of all energy supplied to and dissipated from a mode over a period $\sum \Delta E$ in relation to the amplitude $\hat{q}$ and the modal parameters (frequency $\omega_{0,i}$, modal damping D_i, mass normalized

modal amplitude $\varphi_{i,j}$ at the excitation point j of the considered mode i). In most cases, the introduced energy is determined approximately by linearizing the nonlinear force characteristic at the operating point [11]. The resulting linearized damping from the contact can thus be determined via

$$D_{\mathrm{sl},i} = \frac{\varphi_{i\mathrm{j}}^2 F \frac{d\mu}{dv}(v_0)}{2\omega_{0,i}}. \tag{3}$$

Assuming only a constant modal damping (structural damping) D_i in addition to the linearized energy/damping resulting from the contact, the combination of Equations 1, 2, and 3 leads to the effective damping curves that are equivalent to the nonlinear contact forces characteristic as shown in Figure 1. Figure 1 shows the influence of different parameters on the resulting effective damping. Furthermore, the effective damping gives a direct indication on the stability of the mode under consideration. If the effective damping is positive ($D_{\mathrm{eff},i} > 0$), more energy is dissipated than added, the mode is stable thus the amplitude would decrease. If the effective damping is negative ($D_{\mathrm{eff},i} < 0$), more energy is supplied than dissipated, the mode is unstable, and the amplitude increases.

Thus, a direct relationship exists between the force characteristic consisting of various force components, the effective damping/stability of the system and the resulting amplitude change of the critical mode.

3 Identifying the root cause of self-excited vibrations

To identify and further quantify the root cause of the self-excited vibrations, the self-excitation mechanism and the nonlinear contact force characteristic needs to be determined. Most existing methods to characterize contact pairs and the resulting self-excitation are based on extensive parameter investigations. One way is to determine stability maps by tracking certain operational parameters during operation to identify their stability [12]. This testing of arbitrary operational parameters is data and time consuming. Furthermore, the root-cause of the self-excitation, the nonlinear contact force characteristic is not detected. To determine the nonlinear contact forces, quasi-static tests are usually performed. Here, the average contact force is measured with respect to various speeds in order to generate a static force characteristic [13]. However, the resulting force characteristic can be different from the root cause of the self-excitation, as this is accompanied by both a different time scale (quasi static to natural frequency of the mode) and a variation in velocity, which can have a major impact, especially when interacting with fluid forces, due to the velocity dependence. To characterize and quantify the root cause of self-excitation and determine suitable stable operational parameter sets, a method based on operational data is presented [11]. The nonlinear force characteristic is determined by combining the energy input of the self-excited mode in operation using high-frequency data with the modal information of the excited mode and the instantaneous operational parameters. Therefore, it is necessary to determine the energy change and thus the effective damping from time domain data. Figure 2 left shows a time section of a simulation of a modal reduced order model [14]

$$\ddot{\mathrm{q}}_i(t) + 2\mathrm{D}_i\omega_{0,i}\dot{\mathrm{q}}_i(t) + \omega_{0,i}^2\mathrm{q}_i(t) = \varphi_{i,j}F\mu\left(v_{\mathrm{avg}} + \varphi_{i,j}\dot{q}_\iota(t)\right) \tag{4}$$

whose mean velocity v_{avg} and therefore the velocity in contact increases linearly. This linear change in velocity causes the nonlinear force characteristic $F\mu\left(v_{\mathrm{avg}} + \varphi_{i,j}\dot{q}_\iota(t)\right)$ responsible for the self-excitation to be traversed, resulting in information over a wide range of the characteristic curve. Using simple equations such as the logarithmic decrement

$$D_{\mathrm{eff},i} = \frac{\ln\left(\frac{\hat{x}(t)}{\hat{x}(t+T)}\right)}{\sqrt{4\pi^2 + \ln\left(\frac{\hat{x}(t)}{\hat{x}(t+T)}\right)^2}} \tag{5}$$

or by applying kalman filters [15], the effective damping is determined from the change in amplitude $\hat{x}(t)$ over one vibration period T. Figure 2 right shows this effective damping as a function of the velocity in the

contact. Here it can be clearly seen that from an angular velocity of 17.5 $\frac{rad}{s}$, the effective damping is greater than zero, thus the system is stable. This leads to a decrease of the amplitude of the critical oscillation.

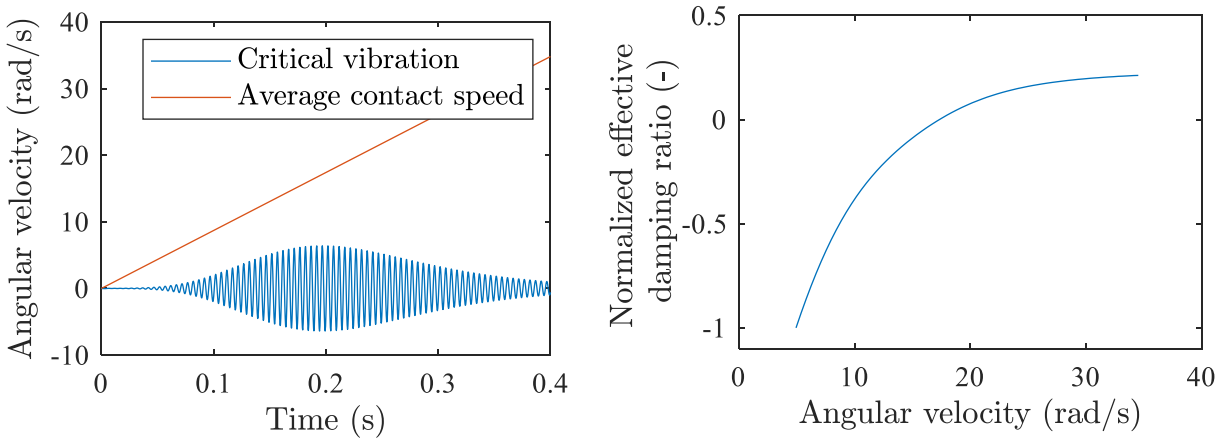

Figure 2: Time domain simulation of a self-excited ROM (left) and corresponding effective damping ratio (right)

From the effective damping $D_{\mathrm{eff},i}$ of the considered mode i, the damping resulting from the self-excitation $D_{\mathrm{s},i}$ can be determined via

$$D_{\mathrm{s},i} = D_{\mathrm{eff},i} - D_i \tag{6}$$

by estimating or determining e.g. experimentally the modal damping D_i. This damping is now directly dependent on the modal parameters and the slope of the nonlinear force characteristic. Equation 3 could be used to directly determine the slope of the force characteristic with respect to various operational parameters (normal force F, velocity in contact v). However, since the characteristic curve is nonlinear and this procedure requires a significant vibration amplitude, the results from Equation 3 are inaccurate, due to the linearization. Therefore, it is necessary to consider the amplitude of the critical vibration. Using

$$\Delta E_{s,i} = \int_0^{\frac{2\pi}{\omega_{0,i}}} F\mu\left(v_0 + \hat{v}\cos\left(\omega_{0,i}t\right)\right)\hat{v}\cos\left(\omega_{0,i}\,t\right)dt, \tag{7}$$

the energy supplied or dissipated in the contact is determined, considering the nonlinear hysteresis which depends on the velocity amplitude of the critical vibration $\hat{v} = \varphi_{i,j}\omega_{0,i}\hat{q}$. This allows the effective damping to be determined dependent on the velocity and amplitude of the vibration (Figure 3).

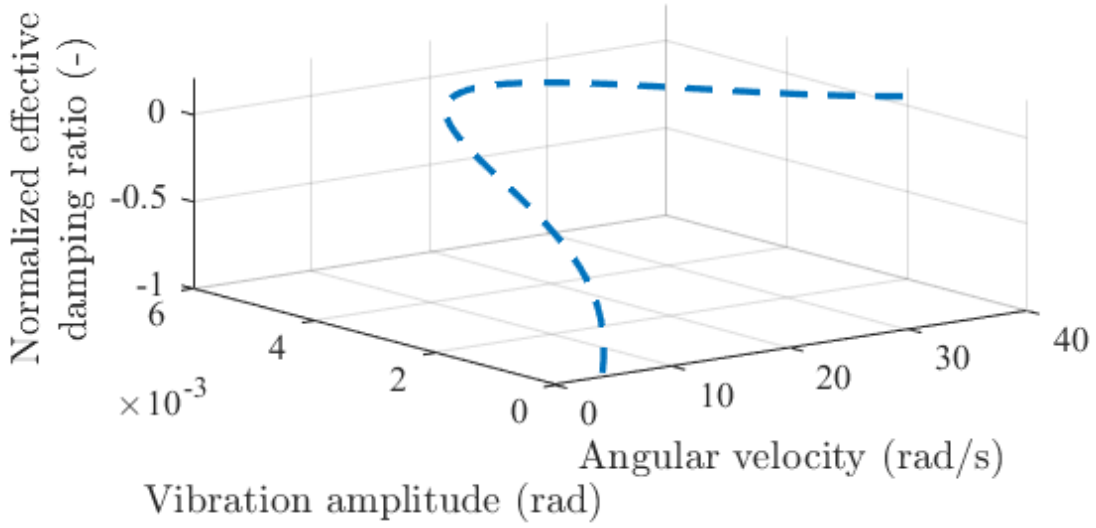

Figure 3: Normalized effective damping ratio with respect to the speed and amplitude in the contact

By substituting Equation 7 in Equation 2, the damping component of the contact force characteristic can be determined via

$$D_{s,i} = \frac{\int_{t_0}^{t_0+T} F\mu(v_0+\varphi_{i,1}\dot{q}_i)\varphi_{i,1}\dot{q}_i dt}{2\omega_{0,i}\int_{t_0}^{t_0+T}\dot{q}_i^2\, dt}. \tag{8}$$

Buy adjusting Equation 8 with an unknown $\mu(v)$ with the determined damping from Equation 6 via the least square method, the slope of the contact force characteristic is determined. Using an operating point (e.g. average force and speed), a contact force characteristic is obtained which agrees very well, both qualitatively and quantitatively, with the characteristic specified in the simulation (Figure 4 left).

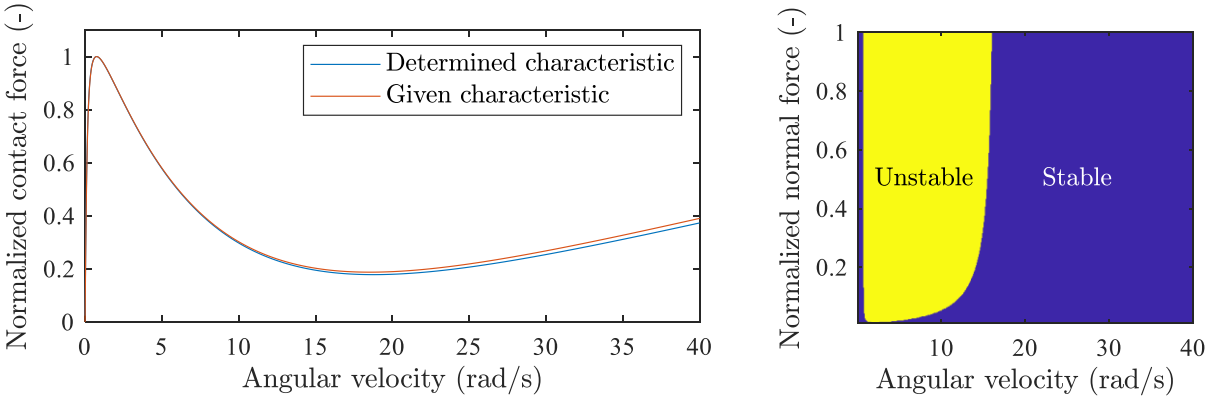

Figure 4: Contact force characteristic determined using the presented method and given in the simulation (left) and corresponding stability map (right)

Through this determination of the contact force characteristic from operational data, the stability of the critical oscillations can now be determined by e.g. using Equation 3 and specially developed stability maps can be generated (Figure 4 right), that take into account amplitude dependent nonlinearities as well as the various effects on the associated time scale.

4 Application to self-excited high-frequency torsional oscillations in downhole drilling systems

Finally, the presented method is applied to self-excited high-frequency torsional oscillations occurring during the drilling process in hard and dense formations. The BHA used in the case studies is of 9 1/2-inch tool size comprised of a PDC bit, a rotary steerable system, stabilizers, formation evaluation tools, mud pulse telemetry tool and a measure-while-drilling (MWD) tool for vibration and load measurement. Figure 5 shows the simplified BHA geometry and the characteristic stick/slip mode and the critical high-frequency torsional drill string modes that occur during the drilling process.

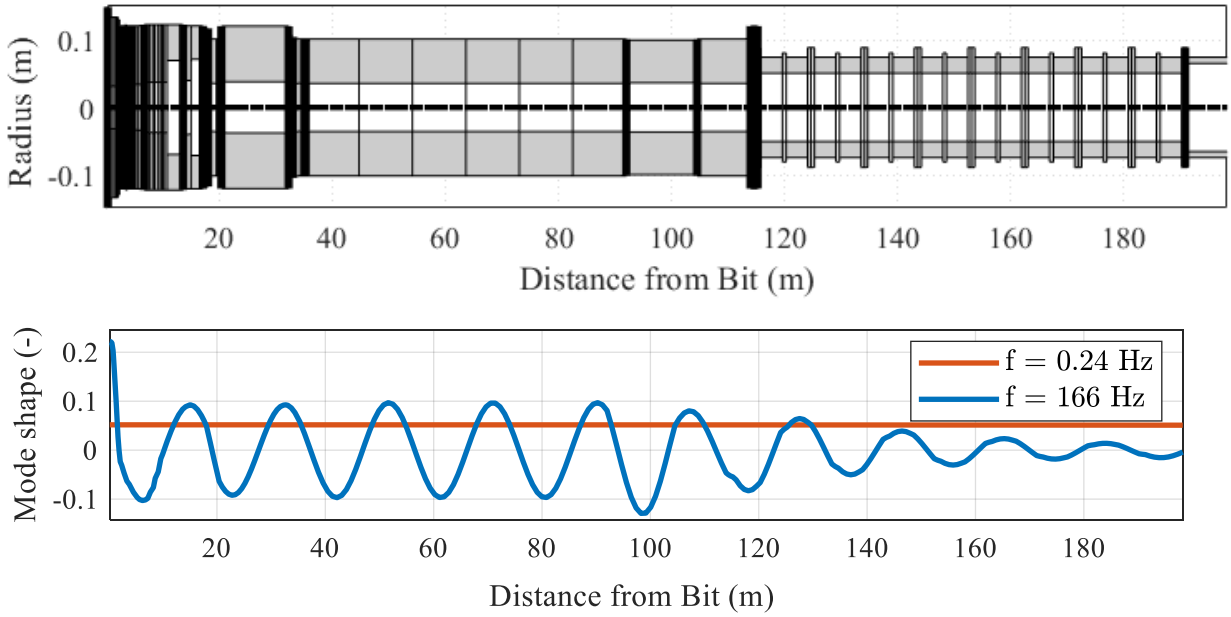

Figure 5: Simplified geometry of a BHA (top) and critical BHA modes (bottom)

Figure 6 top shows a snapshot of measurement data in the time domain recorded by the MWD tool placed close to the bit. Figure 6 bottom shows the velocity divided into the low frequency stick/slip and the high frequency HFTO component. It is evident that the HFTO amplitude increases during the slip phase due to the self-excitation. At some point, the velocity in the slip phase is so high that the fluid forces increase the effective damping and thus the unstable HFTO mode becomes stable, causing the amplitude to decrease again (cf. [16]). The interaction of HFTO and stick/slip is very suitable for the determination of the torque characteristic in the bit-rock interaction, since, as in Figure 2, the change of the low-frequency or average velocity characterizes a broader range of the torque characteristic. Due to the repeated change of the angular velocity at the bit caused by stick/slip as well as the large number of slip phases, a multitude of data is available to determine the torque characteristic responsible for the self-excitation using the presented method. As before, the effective damping is determined for different angular velocities in order to determine the slope of the torque characteristic using Equation 7.

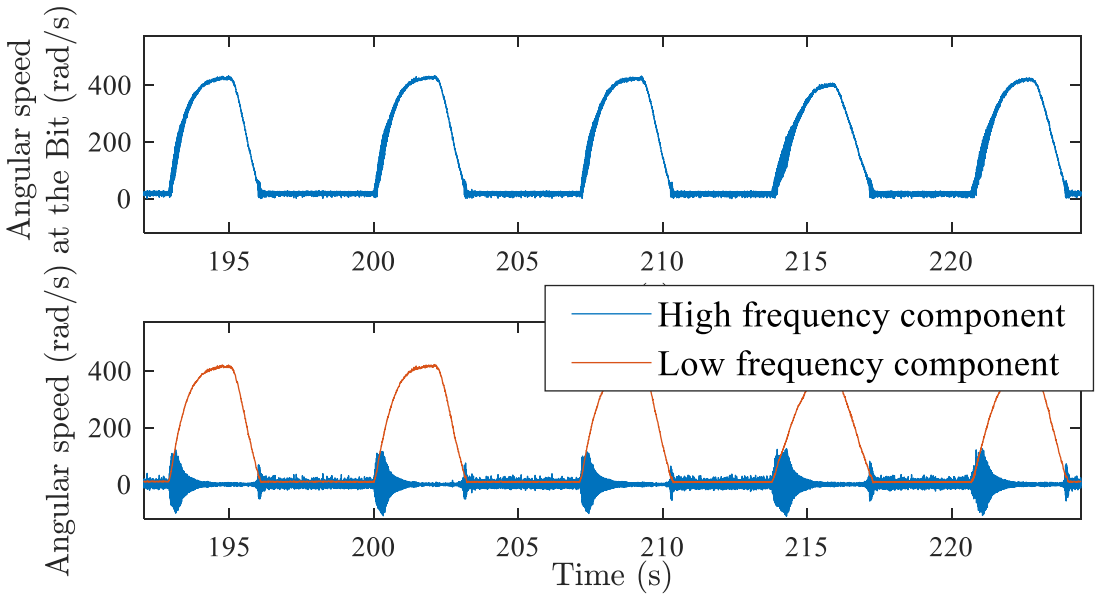

Figure 6: Angular speed at the Bit (top) and corresponding low and high frequency component (bottom)

Figure 7 left shows the normalized effective damping determined from downhole measurement data for different slip phases. Figure 7 right shows the corresponding average normalized torque characteristic determined from the measurement data.

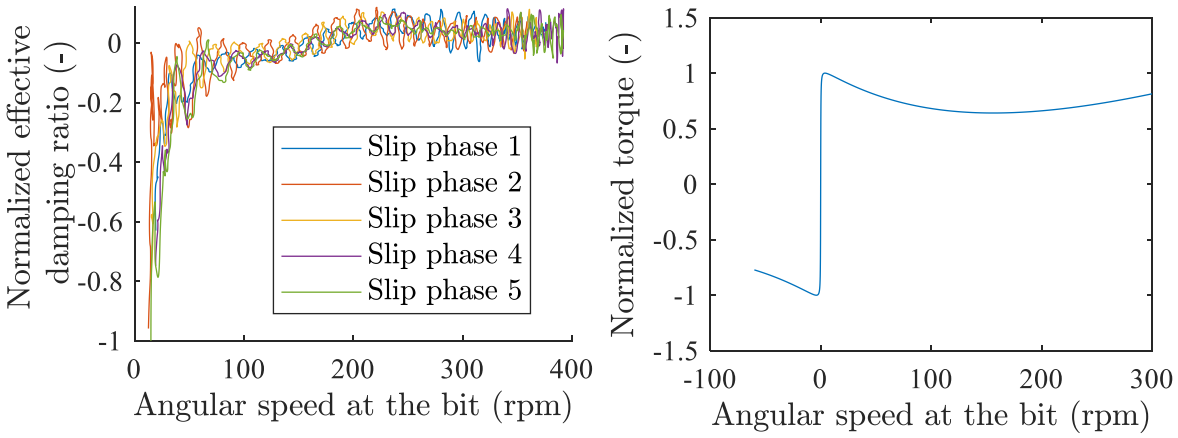

Figure 7: Normalized effective damping ratio in various slip phases (left) and resulting normalized torque characteristic in the bit-rock contact (right)

This torque characteristic can now be used, similar to [11], to determine the stability maps. By reducing the normal force in the contact (weight on bit (WOB)) the slope of the torque characteristic is reduced, thus the energy input is reduced. Furthermore, buy reducing the average speed, the maximum possible amplitude of the disturbance displacement is reduced [17]. Additionally, increasing the relative velocity in the contact can stabilize the system due to the fluid component that is increasing linearly. In addition, the method described here enables different dampers to be taken into account directly with regard to their effect cf. [18, 19] to the effective damping and the stability maps.

5 Conclusion

In this paper, a method to describe the root cause of cutting or friction induced vibrations, the nonlinear contact force characteristic, is presented. By combining the energy input/output into the self-excited mode determined from amplitude changes using measurement data and the modal information of the critical mode, the effective damping of the critical mode is determined. It is shown that the effective damping is equivalent to the nonlinear contact force characteristic.

Furthermore, by relating the resulting effective damping to contact and operational parameters such as normal force and contact velocity as well as modal parameters such as amplitude, mode shape and natural frequency, the nonlinear force characteristic is determined. The nonlinear force characteristic represents the nonlinear forces resulting from the contact responsible for the self-excitation and its parameter dependencies. With this new information, suitable techniques can be developed to reduce unwanted self-excited vibrations.

The presented method was applied to high-frequency torsional vibrations in downhole drill strings to evaluate possible actions to reduce the self-excited vibrations. The method presented here can further be applied to arbitrary self-excited oscillations where the excitation mechanism can be described by a nonlinear force characteristic.

Acknowledgements

The authors would like to thank Baker Hughes for supporting the work and giving permission to publish this paper.

References

[1] J. P.T. Mo, S. C.P. Cheung, and R. Das, “Mechanical Vibration,” in *Demystifying Numerical Models*: Elsevier, 2019, pp. 209–233.

[2] W. J. Bottega, *Engineering Vibrations*. Boca Raton, FL: CRC Press, 2006.

[3] N. M. Kinkaid, O. M. O'Reilly, and P. Papadopoulos, “Automotive disc brake squeal,” *Journal of Sound and Vibration*, vol. 267, no. 1, pp. 105–166, 2003, doi: 10.1016/S0022-460X(02)01573-0.

[4] G.-P. Ostermeyer, “On Tangential Friction Induced Vibrations in Brake Systems,” *SAE Int. J. Passeng. Cars – Mech. Syst.*, vol. 1, no. 1, pp. 1251–1257, 2009, doi: 10.4271/2008-01-2580.

[5] K. Magnus, K. Popp, and W. Sextro, *Schwingungen*. Wiesbaden: Springer Fachmedien Wiesbaden, 2016.

[6] G. Ostermeyer, “Dynamic Friction Laws and Their Impact on Friction Induced Vibrations,” in *SAE Technical Paper Series*, 2010.

[7] C. Glocker, E. Cataldi-Spinola, and R. I. Leine, “Curve squealing of trains: Measurement, modelling and simulation,” *Journal of Sound and Vibration*, vol. 324, 1-2, pp. 365–386, 2009, doi: 10.1016/j.jsv.2009.01.048.

[8] Z. Dombovari, A. Iglesias, M. Zatarain, and T. Insperger, “Prediction of multiple dominant chatter frequencies in milling processes,” *International Journal of Machine Tools and Manufacture*, vol. 51, no. 6, pp. 457–464, 2011, doi: 10.1016/j.ijmachtools.2011.02.002.

[9] A. Hohl *et al.*, “Derivation and experimental validation of an analytical criterion for the identification of self-excited modes in drilling systems,” *Journal of Sound and Vibration*, vol. 342, pp. 290–302, 2015, doi: 10.1016/j.jsv.2015.01.002.

[10] A. Hohl *et al.*, “Prediction and Mitigation of Torsional Vibrations in Drilling Systems,” in *IADC/SPE Drilling Conference and Exhibition*, Fort Worth, Texas, USA, 2016.

[11] V. Kulke, G.-P. Ostermeyer, H. Reckmann, and A. Hohl, “Determination of Operational Parameters to Mitigate HFTO Based on Algorithmic Analysis of Downhole Sampled High-Frequency Data,” in *Day 1 Tue, March 08, 2022*, Galveston, Texas, USA, 2022, p. 168.

[12] C. Herbig *et al.*, “Drillpipe Influence on Drilling Performance,” in *Day 3 Thu, March 19, 2015*, London, England, UK, 2015.

[13] J. F. Brett, “The Genesis of Bit-Induced Torsional Drillstring Vibrations,” *SPE Drilling Engineering*, vol. 7, no. 03, pp. 168–174, 1992, doi: 10.2118/21943-PA.

[14] A. Hohl, V. Kulke, and G.-P. Ostermeyer, “Insights through Modal Minimal Models for Analysis of Linear and Nonlinear Dynamic Problems,” *Shock and Vibration*, vol. 2022, pp. 1–8, 2022, doi: 10.1155/2022/6888399.

[15] M. Ichaoui, G.-P. Ostermeyer, M. Tergeist, and A. Hohl, “Estimation of High-Frequency Vibration Loads in Deep Drilling Systems Using Augmented Kalman Filters,” in *Volume 7A: Dynamics 2020*.

[16] A. Hohl, V. Kulke, A. Kueck, C. Herbig, H. Reckmann, and G.-P. Ostermeyer, “The Nature of the Interaction Between Stick/Slip and High-Frequency Torsional Oscillations,” in *IADC/SPE International Drilling Conference and Exhibition*, Galveston, Texas, USA, 2020.

[17] A. Hohl *et al.*, “Best Practices for Operations in HFTO Prone Applications,” in *SPE Asia Pacific Oil & Gas Conference and Exhibition*, Virtual, 2020.

[18] A. Hohl, V. Kulke, G.-P. Ostermeyer, A. Kueck, V. Peters, and H. Reckmann, “Design and Field Deployment of a Torsional Vibration Damper,” in *IADC/SPE International Drilling Conference and Exhibition*, Galveston, Texas, USA, 2022.

[19] V. Kulke, G.-P. Ostermeyer, M. Tergeist, and A. Hohl, “Semi-Analytical Approach for Derivation of an Equivalent Modal Friction-Damping Ratio and its Application in a Self-Excited Drilling System,” in *Volume 4: Dynamics, Vibration, and Control*, Salt Lake City, Utah, USA, 2019.